RSC Advances

ROYAL SOCIETY OF CHEMISTRY

www.rsc.org/advances

Cite this: DOI: 10.1039/c0xx00000x

www.rsc.org/xxxxxx

Communication

Electrochemically fabricated flower-like graphene as highly efficient Pt electrocatalysts support for methanol oxidation

Qiang Zhang, Fengxing Jiang*, Ruirui Yue, Yukou Du*

Received (in XXX, XXX) Xth XXXXXXXXX 200X, Accepted Xth XXXXXXXXX 200X
DOI: 10.1039/b000000x

The graphene with a well-defined flower-like structure, for the first time, has been fabricated by a facile electrochemical method, which is explored as the support of Pt catalyst for methanol electro-oxidation. The results demonstrate that the Pt-modified flower-like graphene (Pt/*f*-RGO) catalyst performs remarkable electrocatalytic activity (1198.6 mA mg-1$_{Pt}$)

Graphene, a flexible two-dimensional (2D) carbon material with single-atom thickness, has attracted immense attention as a substrate or an electroactive center due to its low cost, large specific surface area, high electrical conductivity and fascinating mechanical properties.[1,2] A large specific surface area is significant for graphene in the fields of supercapacitor, electrochemical sensor and fuel cell applications, which can provide more catalytic adsorption and/or active reaction sites.[3-5] As we know, graphene sheets show a strong tendency to agglomerate due to the enormous Van der Waals forces between layers, which lead to a great decrease of surface area and restrict its promising applications.[6] In order to avoid this weakness, considerable efforts have been made to synthesize three-dimensional (3D) porous graphene materials by various techniques such as chemical vapor deposition (CVD), aerogel, hydrogel methods and so on.[7-10] The 3D porous graphene shows large specific surface area, good flexibility and excellent electrochemical properties in practical applications.[1,11] However, these methods involve the advanced equipments, the exacting terms or the complicated preparation processes such as high temperature, high-quality substrate materials or accurate control over cooling rates.[4] Therefore, it is highly desired that a facile and feasible method could be developed to prepare the 3D porous graphene.

In this communication, we report a facile electrochemical method to fabricate the well-defined flower-like reduction graphene oxide (*f*-RGO) with 3D porous structure for the first time to the best of our knowledge. As electrocatalyst support, the *f*-RGO remarkably enhances the electrocatalytic activity of Pt nanoparticles compared to the graphene-supported Pt catalysts on glassy carbon electrode (GCE) toward methanol oxidation. This work presents a new attempt to use the 3D porous *f*-RGO supports for the development of highly efficient Pt/*f*-RGO electrocatalysts.

The entire synthesis of *f*-RGO modified GCE (*f*-RGO/GCE) was carried out via a simple electrochemical method. Frist, graphene oxide (GO) was firstly synthesized by exfoliating graphite power via a modified Hummers' method;[12] And then, 5 mg GO product was thoroughly dispersed in 10 mL deionized water. 10 μL GO suspension was uniformly dropped on the surface of GCE. The reduction of GO was conducted potentiostatically in Na–PBS solution (Na_2HPO_4/NaH_2PO_4, 0.01 M, pH =4.12) at -0.9 V for 2000 s; Second, a certain amount of Cu nanoparticles were electro-deposited on the prepared RGO layer at -0.4 V in 5.0 mM $CuSO_4$ solution; After that, anther 10 μL GO suspension by the same electrochemical reduction procedure was added on the electrode surface to prepare a sandwich construction of RGO/Cu/RGO on the surface of the electrode. The resulting electrode was kept into Na–PBS solution

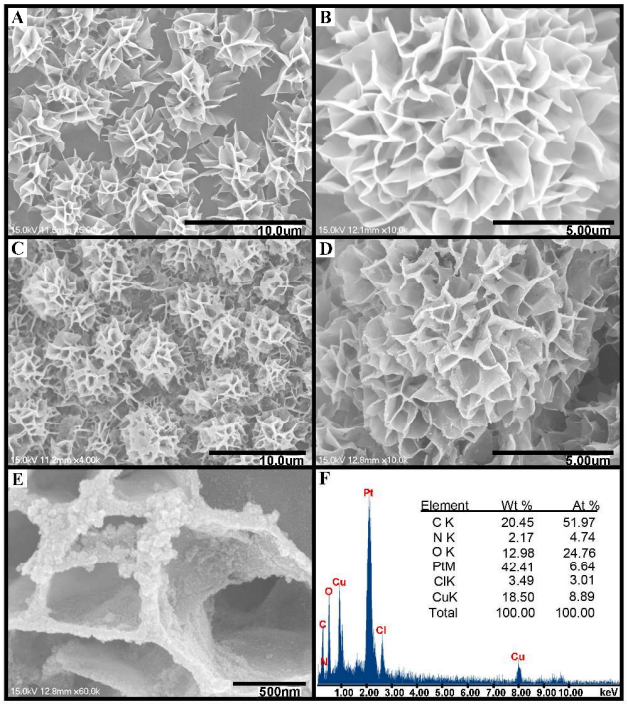

Fig. 1 SEM images of *f*-RGO/GCE (A and B), Pt/*f*-RGO/GCE (C-E), and EDX spectra of Pt/*f*-RGO/GCE (F).

under a positive potential of 0 V for 1000 s to remove Cu nanoparticles thoroughly and was denoted as *f*-RGO/GCE. For the preparation of electrodes, the same amounts of GO ink (20 μL) was dropped on the bare GCE and allowed to dry in air; Finally, a required amount of $H_2PtCl_6{\cdot}6H_2O$ (1.5 mM, 4.0 μL) was dropped onto the surface of *f*-RGO/GCE, and then 6.0 μL of freshly prepared $NaBH_4$ (10 mM) solution was added to obtained Pt nanoparticles. After that the modified electrode (*f*-RGO/GCE) was rinsed several times with deionized water and ethanol to remove all excess $NaBH_4$. For comparison, the same amount of Pt nanoparticles modified RGO/GCE and bare GCE were prepared by the similar method stated above, and the prepared electrodes were denoted as Pt/RGO/GCE and Pt/GCE, respectively. The mass loading of Pt on all electrodes was fixed the same with a value of 0.00117 mg. Meanwhile, the mass of the obtained RGO was estimated to be 0.01 mg on the surface of Pt/*f*-RGO/GCE and Pt/RGO/GCE.

The electrochemical experiments were performed on a CHI 660B electrochemical workstation (Shanghai Chenhua Instrumental Co., Ltd., China) using a standard three-electrode-cell equipped with a catalyst modified GCE (3.0 mm in diameter), a platinum wire and a saturated calomel electrode (SCE) as the working, counter and reference electrode, respectively. The electrochemical properties were performed with cycle voltammetry (CV) and CA in the solution of 0.5 M H_2SO_4 without or with CH_3OH at 50.0 mV s^{-1} at room temperature. CO stripping voltammetry was tested by the oxidation of pre-adsorbed CO in 0.5 M H_2SO_4.

The morphologies of the as-prepared *f*-RGO without and with Pt nanoparticles have been characterized by SEM (Fig. 1A-E). As observed in Fig. 1A, the graphene framework has a well-defined and uniformly distributed flower-like structure on the GCE. Meanwhile, the *f*-RGO exhibits the typical porous architectures (Fig. 1B), which may be a good candidate as the support material in fuel cells.[13, 14] As seen from Fig. 1C-D, *f*-RGO appears to have a rough morphology with uniform Pt grains located on the surface of each RGO petal. From the enlarged SEM image (Fig.1E), it is obviously that the surface of *f*-RGO is rough with many nanoparticles coated on. In comparison with the smooth surface of the pure *f*-RGO shown in Fig.2A and B, the rough surface of *f*-RGO in Fig.2C and D indicates the presence of Pt nanoparticles, which can be further confirmed by the EDX characterization.The EDX (Fig. 1F) analysis performs that the mass loading of Pt on Pt/*f*-RGO/GCE is about 42.4 wt%. It is well-known that the porous structures of graphene provide a larger surface area compared with the common plane graphene, which can effectively promote the dispersion of Pt nanoparticles.

In our experiments, the Pt/*f*-RGO fragments scraped from Pt/*f*-RGO/GCE were thoroughly crushed and dispersed in deionized water for TEM characterization. Fig. 2A-C show TEM images and the corresponding histogram of particle size distribution for the Pt/*f*-RGO/GCE catalyst. The TEM images of Pt/*f*-GRO/GCE (Fig.2A and B) show that the Pt particles are in nanoscale, which follows the normal distribution (Fig. 2C). As the TEM images exhibited, Pt nanoparticles with a mean particle size of 3.14± 1.05 nm are well-dispersed on the surface of *f*-RGO without obvious aggregations, which is particularly desirable to electrocatalytic performance towards methanol oxidation. Meanwhile, the corresponding TEM images of Pt/RGO and Pt catalysts are recorded in Fig. S1. Since it is difficult for Pt/*f*-RGO/GCE sample to carry out XRD measurements, and similar Pt/*f*-RGO can also be formed on carbon cloth (CC), therefore, Pt/*f*-RGO coated on the surface of CC (denoted as Pt/*f*-RGO/CC) instead of Pt/*f*-RGO/GCE was used for XRD characterization (Fig. 2D). Fig. 2D shows the XRD patterns of the Pt/CCE, Pt/RGO/CCE and Pt/*f*-RGO/CCE. The peaks at around 39.9°, 46.6°, 67.7°, 81.7°, and 86.1° are attributed to the diffraction peaks of crystal faces Pt(111), (200), (220), (311), and (222),[15] respectively. However, how does the *f*-GRO structure form? We analyses as that the formation of the *f*-GRO has relation to the process of removing the Cu particles. There may be electrostatic interactions between the RGO layers and the moving Cu^{2+} ions. Besides the electrostatic interaction, impact force as well as resistance with Cu^{2+} ions transporting through the GE layer may also contribute to the formation of *f*-RGO.

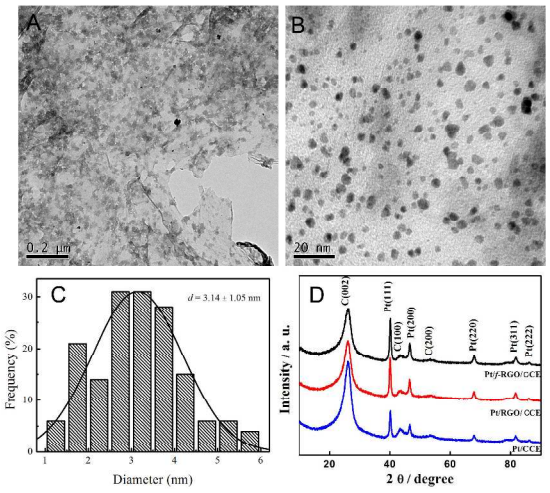

Fig. 2 TEM images of Pt/*f*-RGO/GCE (A and B); diameter size distribution (C) obtained from B; XRD patterns of Pt/*f*-RGO/CCE, Pt/ RGO/CCE and Pt/CCE (D).

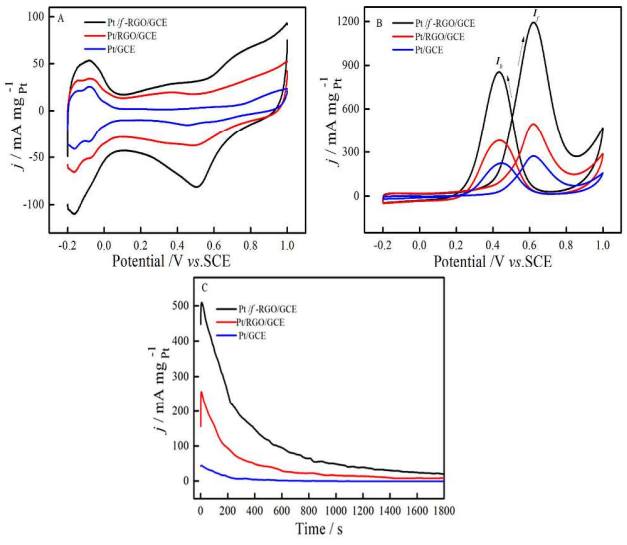

Fig. 3 (A) CVs of Pt/*f*-RGO/GCE, Pt/RGO/GCE and Pt/GCE in 0.5 M H_2SO_4 solution without (A) and with (B) 1.0 M methanol at 50.0 mV s^{-1}; (C) CA of Pt/*f*-RGO/GCE, Pt/RGO/GCE and Pt/GCE at 0.5 V in 1.0 M CH_3OH + 0.5 M H_2SO_4 solution.

Fig. 3A shows the representative cyclic voltammograms (CVs)

of Pt/*f*-RGO/GCE, Pt/RGO/GCE and Pt/GCE catalysts measured in a nitrogen-saturated 0.5 M H_2SO_4 solution. The CVs profiles present the typical hydrogen adsorption/desorption ($H_{ads}/_{des}$) peaks (-0.25~0.1 V), electrochemical double-layer (0.1~0.25 V) and reduction peaks for platinum oxide (0.4~0.6 V). Obviously, Pt/*f*-RGO/GCE presents the largest hydrogen adsorption/desorption area compared to that of Pt/RGO/GCE and Pt/GCE, which is coincident with the largest reduction peaks of the electrocatalyst. It is due to the porous structure of *f*-RGO on GCE and the well-dispersed Pt nanoparticles on it. The *ECSA* based on the area of $H_{ads}/_{des}$ peaks was denoted as $ECSA_H$, and were recorded in Table 1. It can be found that the $ECSA_H$ decrease in the order of Pt/*f*-RGO/GCE (79.8 m^2 g^{-1}) > Pt/RGO/GCE (51.3 m^2 g^{-1}) > Pt/GCE (21.5 m^2 g^{-1}), indicating that the Pt/*f*-RGO/GCE will show a higher electrocatalytic activity. Moreover, electrochemical active surface area (*ECSA*) of GCE, RGO/GCE, *f*-RGO/GCE were also calculated (Fig. S2). Hence, the larger ECSA of Pt/*f*-RGO/GCE results in the higher double layer capacitance of Pt/*f*-RGO/GCE as compared to other electrodes.[16,17] For investigating the electrocatalytic activity of catalysts for methanol oxidation, the CVs were conducted in the solution of 1.0 M CH_3OH + 0.5 M H_2SO_4 solution in Fig. 3B. All the CVs show two well-defined methanol oxidation peaks, one is the forward peak at about 0.63 V and the other is the backward peak at 0.45 V. Obviously, the mass peak density in the forward peak (I_f) has the largest value of 1198.6 mA mg^{-1}_{Pt} on Pt/*f*-RGO/GCE in Table 1, which is ~2.41 times and ~4.32 times higher than those on Pt/RGO/GCE (496.9 mA mg^{-1}_{Pt}) and Pt/GCE (277.5 mA mg^{-1}_{Pt}), respectively. It suggests that the *f*-RGO remarkably enhances the electrocatalytic activity of Pt nanoparticles toward methanol oxidation due to the large *ECSA* of Pt/*f*-RGO/GCE, which is in agreement with the results of $ECSA_H$. On the other hand, Fig. 3C presents the stability of catalysts for methanol oxidation by CA at 0.5 V for 1800 s. At the initial stage, the mass current densities on all the catalysts display rapid decay, which is attributed to the accumulation of intermediate CO-like species on the surface of Pt nanoparticles during the methanol oxidation reaction.[18-21] However, the Pt/*f*-RGO/GCE always exhibits a higher mass current density during the whole 1800 s process as compared with Pt/RGO/GCE and Pt/GCE. At the end of the test, the oxidation current density at Pt/*f*-RGO/GCE is 23.24 mA mg^{-1}_{Pt}, which is about 2.0 times and 19.4 times higher than those on Pt/RGO/GCE (11.57 mA mg^{-1}_{Pt}) and Pt/GCE (1.21 mA mg^{-1}_{Pt}), respectively. Furthermore, we also recorded 500 cycles of CV for Pt/*f*-RGO/GCE, Pt/RGO/GCE and Pt/GCE in 1.0 M CH_3OH + 0.5 M H_2SO_4 solution at 0.5 V in Fig. S3. As observed from Fig. S3, methanol oxidation on Pt/*f*-RGO/GCE exhibits higher mass current density than that of Pt/RGO/GCE and Pt/GCE during the whole 500 cycles. After operation for 500 cycles, the current density of methanol oxidation on Pt/*f*-RGO/GCE is still higher than that of Pt/RGO/GCE and Pt/GCE.

Table 1 Electrochemical parameters of as-prepared catalysts.

Catalysts	Q_H /mC	$ECSA_H$ / m^2 g^{-1}	I_f /mA mg^{-1}	Q_{CO} /mC	$ECSA_{CO}$ /m^2 g^{-1}	E_{CO} /V
Pt/*f*-RGO/GCE	0.194	79.8	1198.6	0.501	88.4	0.66
Pt/RGO/GCE	0.127	51.3	496.9	0.328	57.8	0.66
Pt/GCE	0.053	21.5	277.5	0.136	23.9	0.77

To further investigate the catalytic activity of catalysts, the CO stripping voltammtrey was performed in 0.5 M H_2SO_4 solution. As seen from Fig. 4, the Pt/*f*-RGO/GCE displays a similar peak potential of CO_{ads} oxidation (E_{CO}=0.66 V) with the Pt/RGO/GCE, which is lower than that on Pt/GCE (0.77 V). The negative shift of E_{CO} on Pt/*f*-RGO/GCE indicates a good CO poisoning tolerance.[22] In addition, the *ECSA* based on the CO_{ads} oxidation ($ECSA_{CO}$) on catalysts were estimated and recorded in Table 1. It can be found that the Pt/*f*-RGO/GCE catalyst shows the largest

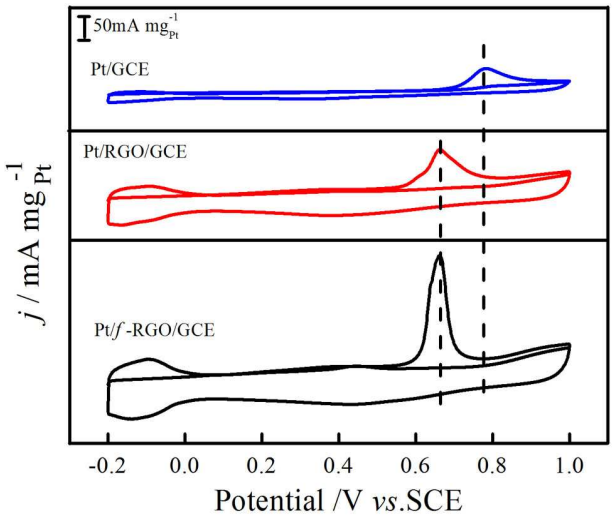

Fig. 4 CO stripping voltammograms of Pt/*f*-RGO/GCE, Pt/RGO/GCE and Pt/GCE in 0.5 M H_2SO_4 solution at 50.0 mV s^{-1}.

charge of CO_{ads} oxidation (Q_{CO}) and $ECSA_{CO}$ (88.4 m^2 g^{-1}), which are well consistent with the results of $ECSA_H$ (Fig. 2A) and further indicates the *f*-RGO to be a promising catalyst support.

In conclusion, we successfully synthesized a flower-like graphene by a facile electrochemical method severing as Pt nanoparticles support for methanol oxidation. The *f*-RGO with the porous structure promotes the homogeneous dispersion and *ECSA* of Pt nanoparticles ($ECSA_{CO}$=88.4 m^2 g^{-1}). The CVs and CA demonstrate that the Pt/*f*-RGO/GCE catalyst shows a higher mass peak current density (1198.6 mA mg^{-1}_{Pt}) and a better stability compared with the common Pt/RGO/GCE and Pt/GCE towards methanol oxidation, respectively. Such an excellent electrocatalytic activity of Pt/*f*-RGO/GCE is mainly ascribed to the large surface area of porous graphene flower. Moreover, CO stripping voltammetry indicates that Pt/*f*-RGO/GC electrode has an excellent CO tolerance. The *f*-RGO could be developed to be a promising electrocatalyst support material for the catalytic application in fuel cells.

This work was supported by the National Natural Science Foundation of China (Grant Nos. 51073114 and 20933007), Suzhou Nano-project (ZXG2012022) and the Priority Academic

Program Development of Jiangsu Higher Education Institutions (PAPD).

Notes and references

College of Chemistry, Chemical Engineering and Materials Science, Soochow University, Suzhou 215123, PR China. Fax: +86 512 65880089; Tel: +86 512 65880361; E-mail: duyk@suda.edu.cn

1. X.D. Huang, K. Qian, J. Yang, J. Zhang, L. Li, C.Z. Yu and D.Y. Zhao, *Adv. Mater.*, 2012, **24**, 4419.
2. G. Kucinskis, G. Bajars and J. Kleperis, *J. Power Sources*, 2013, **240**, 66.
3. Z.Q. Yao, M.S. Zhu, F.X. Jiang, Y.K. Du, C.Y. Wang and P. Yang, *J. Mater. Chem.*, 2012, **22**, 13707.
4. Z.H. Wen, X.C. Wang, S. Mao, Z. Bo, H. Kim, S.M. Cui, G.H. Lu, X.L. Feng and J.H. Chen, *Adv. Mater.*, 2012, **24**, 5610.
5. Z.M. Sheng, C.X. Guo and C.M. Li, *Electrochem. Commun.*, 2012, **19**, 77.
6. S.J. Guo and S.J. Dong, *Chem. Soc. Rev.*, 2011, **40**, 2644.
7. L.G.D. Arco, Y. Zhang, C.W. Schlenker, K. Ryu, M.E. Thompson and C. Zhou, *ACS Nano*, 2010, **4**, 2865.
8. J.L. Vickery, A.J. Patil and S. Mann, *Adv. Mater*., 2009, **21**, 2180.
9. D.Q. Fan, Y. Liu, J.P. He, Y.W. Zhou and Y.L. Yang, *J. Mater. Chem.*, 2012, **22**, 1396.
10. M.A. Worsley, P.J. Pauzauskie, T.Y. Olson, J. Biener, J.H. Satcher, Jr. and T.F. Baumann, *J. Am. Chem. Soc.*, 2010, **132**, 14067.
11. H.P. Cong, X.C. Ren, P. Wang and S.H. Yu, *ACS Nano*, 2012, **6**, 2693.
12. W.S. Hummers and R.E. Offerman, *J. Am. Chem. Soc*., 1958, **80**, 1339.
13. F. Zhao, W.S. Li, W.G. Zhang, F.Q. Sun, Z.H. Zhou and X.D. Xiang, *Int. J. Hydrogen Energy*, 2010, **35**, 8101.
14. C.S. Chen and F.M. Pan, *Appl. Catal.*, B, 2009, **91**, 663.
15 *C.V. Rao, A. Reddy, Y. Ishikawa and P. M. Ajayan, Carbon, 2011,***49**, 931.
16. L. Wang and Y. Yamauchi, *Chem. Mater.*, 2009, **21**, 3562.
17. J. Lu, I.. Do, L.T. Drzal, R.M. Worden and I. Lee, *ACS Nano*, 2008, **2**, 1825.
18. H.M. Zhang, F.X. Jiang, R. Zhou, Y.K. Du, P. Yang, C.Y. Wang and J.K. Xu, *Int. J. Hydrogen Energy*, 2011, **36**, 15052.
19. B.M. Luo, S. Xu, X.B. Yan and Q.J. Xue, Electrochem. Commun., 2012, **23**, 72.
20. A. Kabbabi, R. Faure, R. Durand, B. Beden, F. Hahn, J.M. Leger and C. Lamy, *J. Electroanal. Chem.*, 1998, **444**, 41.
21. R.F. Wang, H.H. Da, H. Wang, S. Ji and Z.Q. Tian, *J. Power Sources*, 2013, **233**, 326.
22. X.C. Zhou, C.P. Liu, J.H. Liao, T.H. Lu and W. Xing, *J. Power Sources*, 2008, **179**, 481.

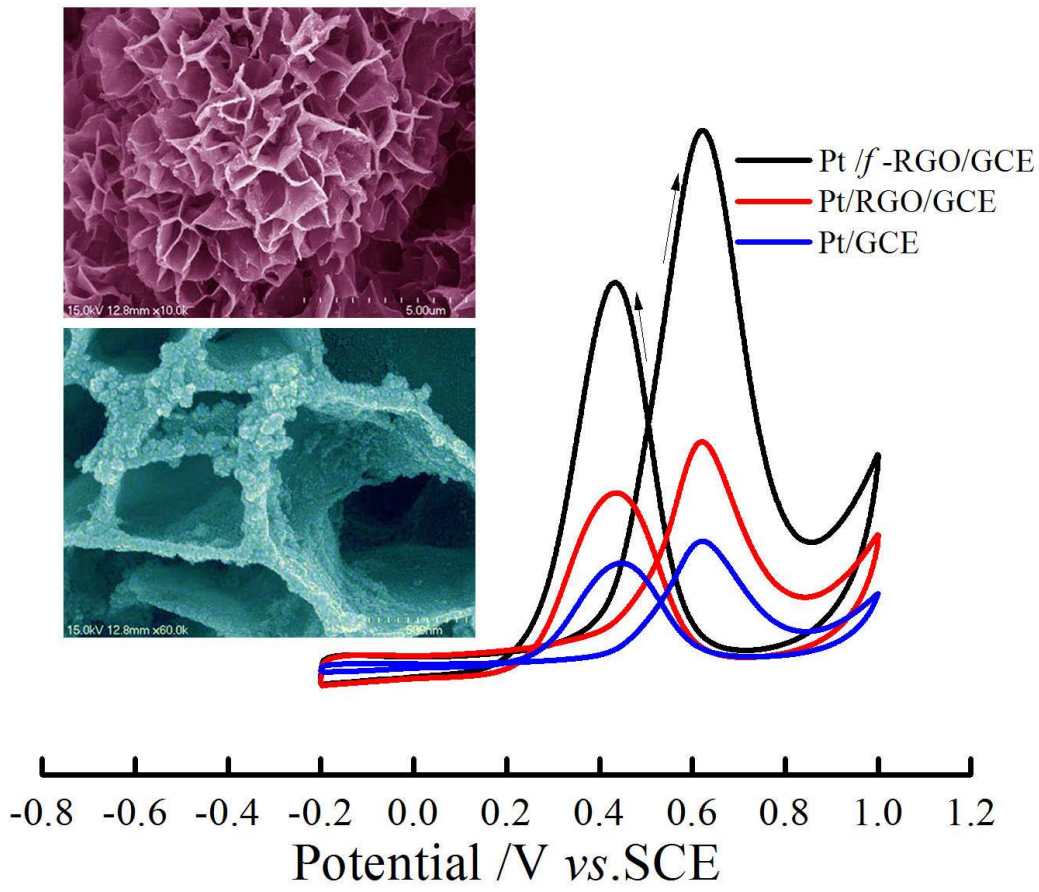

Flower-like graphene (*f*-RGO) with porous was firstly fabricated by an electrochemical method, showing high catalytic activity toward methanol oxidation.